Advances in Radio Science (2004) 2: 101–105

Advances in Radio Science

Integral equation analysis of complex (M)MIC-structures with optimized system matrix decomposition and novel quadrature techniques

T. Vaupel[1] **and V. Hansen**[2]

[1]FGAN-FHR, Neuenahrer Str. 20, 53343 Wachtberg, Germany
[2]Department of Electromagnetic Theory, University of Wuppertal, Germany

Abstract. Using integral equation methods for the analysis of complex (M)MIC structures, the computation and storage effort for the solution of the linear systems of equations with their fully populated matrices still forms the main bottleneck. In the last years, remarkable improvements could be achieved by means of diakoptic methods and related preconditiners. In this contribution, we present a method based on the optimized decomposition of the system matrix depending on the circuit topology. The system matrix is splitted in a densely populated matrix and a mainly blockdiagonal matrix with overlapping submatrices. The latter matrix is used for the generation of high performance preconditioners within Krylov subspace methods using sparsified matrix storage methods, adaptive Cholesky decompositions and optimized forward/backward substitutions. Furthermore, we present an integration technique using a complete analytical treatment for the strongly oscillating parts of the spectral domain integrands allowing the analysis of very large structures as compared to the wavelength.

1 Introduction

For the analysis and design process of (M)MIC structures, integral equation techniques based on the method of moments (MoM) are well suited and widely used. Many new techniques have been introduced for the efficient generation of the system matrix as well as for the computational effort reduction during the solution of the linear systems of equations. However, problems may still occur for large structures as compared to the wavelength and with complex topology. Based on the techniques in (Vaupel and Hansen, 2001)(Vaupel and Hansen, 2002), an optimized system matrix decomposition is now performed leading to high performance preconditioners whereas the application of a Legendre-Filon quadrature allows the versatile treatment of highly oscillatory spectral domain integrands. The basic idea for the optimized system matrix decomposition stems from the experiences with the diakoptics-based MoM implementations given in (Ooms and De Zutter, 1998). The generation of macro basis functions (MBs) is extended to entire domain diakoptic basis functions using block Gauss-Seidel procedures, but we could prove in (Vaupel and Hansen, 2002), that this approach still behaves $\sim O(N^3)$. On the other hand, a direct iterative improvement of the current distribution derived by the MBs using block relaxation processes did not converge (Ooms and De Zutter, 1998). We can show now, that this diverging behavior can be traced back on an insufficient system matrix decomposition used during the relaxation process. We have derived rules leading to an extended system matrix decomposition which guarantees fast convergence within a block Jacobi process and is especially well-suited for high performance preconditioners.

The creation of the system matrix of large structures requires the evaluation of spectral domain integrals with highly oscillatory integrands. To overcome this, several strategies (e.g. Pilz and Menzel, 1999) based on Filon integration principles (Filon, 1928) have been proposed, but they mainly suffer from a low integration order. Thus, we have extended the Gauss-Legendre quadrature by solving small linear systems of equations with modified right hand sides providing integration weights already containing the oscillatory parts of the integrands.

2 Formulation

A typical section of a (M)MIC structure is given in Fig. 1. As already outlined in Vaupel and Hansen (2002), additional ports are introduced, causing a block decomposition of the structure, in this example the ports P1...P4 lead to the blocks B1...B6. Each port is allocated two blocks which are connected with the port basis function. The macro basis functions (MBs) are created by the subsequent excitation of the ports and their allocated blocks in absence of all other blocks.

Correspondence to: T. Vaupel
(vaupel@fgan.de)

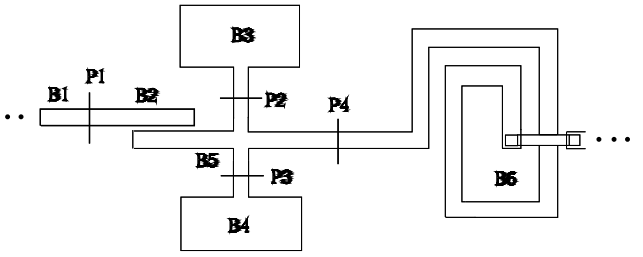

Fig. 1. Section of a typical (M)MIC-structure with port and block numbering.

For example port 3 excites block 3 and block 5. The current profiles on the corresponding blocks (computed with standard MoM) form the MBs. In the next step, we perform an upper level MoM by computing the couplings between the MBs, for example the coupling between the MBs "k" and "l" is computed by

$$Z_{kl} = \sum_{m \in \mathrm{MB}_k} \sum_{n \in \mathrm{MB}_l} I_{mk} Z_{nm} I_{nl} \tag{1}$$

with Z_{nm} the entries of the lower level MoM, $m \in \mathrm{MB}_k$ is the index m of all basis functions allocated to the MB number k, I_{mk} the current profile of the kth MB etc. The Z_{kl} are the entries of the upper level MoM system matrix. Solving for the amplitudes of the MBs and the subsequent superposition of the weighted current profiles of the MBs lead to a first approximation of the overall current distribution, but often the error exceeds 10%. To diminish this error, a block Gauss-Seidel process was proposed (Ooms and De Zutter, 1998), applied to each MB, transforming the original subdomain MB into an entire domain diakoptic basis function within a few iterations. The weighted superposition of the diakoptic basis function provides again the overall current. The error remains below 1% compared to a direct solution, but we could already show (Vaupel and Hansen, 2002), that the overall process is still $\sim O(N^3)$, but is 10–30 times faster than the direct solution.

To reduce this high numerical complexity, a direct improvement of the current distribution $\boldsymbol{I_0}$ provided by the subdomain MBs was proposed, performing the block Jacobi process

$$\mathbf{Z^i} \cdot \boldsymbol{I_{n+1}} = \boldsymbol{U} - \mathbf{Z^c} \cdot \boldsymbol{I_n}, \quad \mathbf{Z} = \mathbf{Z^i} + \mathbf{Z^c} \tag{2}$$

using $\boldsymbol{I_0}$ as start vector.

$\mathbf{Z^i}$ is proposed a sparse block diagonal matrix containing the self and mutual couplings of each block forming diagonal submatrices, whereas $\mathbf{Z^c}$ comprises all remaining mutual couplings.

Unfortunately, this process does not converge in most cases since the convergence condition

$$\rho(\mathbf{Z^{i^{-1}}Z^c}) < 1$$

cannot be fulfilled with the chosen matrix decomposition where $\rho(\mathbf{A})$ denotes the spectral radius of a matrix $\mathbf{A}$.

But we get a convergent Jacobi process by using an appropriate extension of the matrix $\mathbf{Z^i}$ employing the following rule: If block s and block t form together a MB, i.e. it exists a current coupling between the two blocks, then the submatrix $\mathbf{Z_{st}}$ must be added to the matrix $\mathbf{Z^i}$.

For the structure in Fig. 1 we create the following matrix $\mathbf{Z^i}$:

$$\mathbf{Z^i} = \begin{bmatrix} \mathbf{Z_{11}} & \mathbf{Z_{12}} & 0 & 0 & 0 & 0 \\ \mathbf{Z_{21}} & \mathbf{Z_{22}} & 0 & 0 & 0 & 0 \\ 0 & 0 & \mathbf{Z_{33}} & 0 & \mathbf{Z_{35}} & 0 \\ 0 & 0 & 0 & \mathbf{Z_{44}} & \mathbf{Z_{45}} & 0 \\ 0 & 0 & \mathbf{Z_{53}} & \mathbf{Z_{54}} & \mathbf{Z_{55}} & \mathbf{Z_{56}} \\ 0 & 0 & 0 & 0 & \mathbf{Z_{65}} & \mathbf{Z_{66}} \end{bmatrix} \tag{3}$$

We can recognize an additional subdivision of this matrix into three further quadratic submatrices $\mathbf{Z_1} \ldots \mathbf{Z_3}$ where $\mathbf{Z_1}$ comprises the submatrices from $\mathbf{Z_{11}}$ to $\mathbf{Z_{22}}$, $\mathbf{Z_2}$ the submatrices from $\mathbf{Z_{33}}$ to $\mathbf{Z_{55}}$ and $\mathbf{Z_3}$ the submatrices from $\mathbf{Z_{55}}$ to $\mathbf{Z_{66}}$, thus $\mathbf{Z_3}$ overlaps with $\mathbf{Z_2}$ in their common submatrix $\mathbf{Z_{55}}$. We can observe that the topology of the (M)MIC-circuitry is completely transferred to the submatrix decomposition of $\mathbf{Z^i}$. As next step, we perform an adapted Cholesky decomposition of $\mathbf{Z^i}$ using the described submatrix decomposition thus minimizing the number of computational steps. In this context, we can also perform an incomplete Cholesky decomposition to avoid possible fill-ins of matrix entries. The Cholesky decomposition, denoted with $\mathbf{C}$, can be used to perform Eq. (2), but it is much better to use it as left and right preconditioner within Krylov subspace methods, employing the equivalent linear system of equations

$$\mathbf{C^{-1}Z\,C^{-T}C^T} \cdot \boldsymbol{I} = \mathbf{C^{-1}} \cdot \boldsymbol{U}. \tag{4}$$

This results in decisive benefits in contrast to Eq. (2):

- about the same computational effort per iteration as Eq. (2)
- excellent convergence behavior nearly independent on start vector
- No explicit generation of MBs with additional port excitation necessary

$\Rightarrow$ block decomposition also at broad transmission lines, arbitrary structure excitation

- fast convergence also with incomplete Cholesky decomposition.

Another problem arising with large structures is combined with strongly oscillating coupling integrands.

Regarding e.g. the coupling integral of two x-directed basis functions we get

$$Z_{nm} = \int_{k_x=0}^{k_{x,a}} \int_{k_y=0}^{k_{y,a}} G^E_{Jxx} \mathrm{Re}\{F_{m0}(k_x) F_{n0}(k_x) e^{jk_x \Delta x_{nm}}\} \cdot \mathrm{Re}\{F_{m0}(k_y) F_{n0}(k_y) e^{jk_y \Delta y_{nm}}\} dk_x dk_y. \tag{5}$$

Here, F_{m0} ,F_{n0} denote the Fourier transforms of the non-shifted basis functions. The integrand becomes highly oscillatory with large lateral distances Δx_{nm}, Δy_{nm} thus a very

high number of sampling points is necessary using standard quadrature techniques. To overcome this constraint, we employ the following procedure, e.g. outlined for the integration with regard to k_x.

The aim is to integrate

$$\int_a^b f(k_x) e^{jc k_x} dk_x \approx C_{sc} \sum_{j=1}^{N} \tilde{w}_j f(x_j) \tag{6}$$

with $f(k_x)$ typically a smooth function of k_x, $\tilde{w}_j$ integration weights adapted to $e^{jc k_x}$ and x_j appropriate sample points. Using the substitution $k_x(t) = \frac{b-a}{2}t + \frac{a+b}{2}$, $\frac{dk_x}{dt} = \frac{b-a}{2}$, we can introduce the Legendre expansion

$$f(k_x(t)) = \sum_{n=1}^{N-1} a_n p_n(t), t \in [-1, 1] \tag{7}$$

with a_n the expansion coefficients. We can write

$$\int_a^b f(k_x) e^{jc \cdot k_x} dk_x = \int_{-1}^{1} f(k_x(t)) e^{jc \cdot k_x(t)} \frac{dk_x}{dt} dt \approx$$

$$\frac{b-a}{2} e^{j \cdot e} \sum_{n=1}^{N-1} a_n \int_{-1}^{1} p_n(t) e^{jd \cdot t} dt \tag{8}$$

with $d = \frac{c \cdot (b-a)}{2}$, $e = \frac{c \cdot (b+a)}{2}$ and $C_{sc} = \frac{b-a}{2} e^{j \cdot e}$. The best approximation for the integral with the given Legendre expansion is obtained if we achieve

$$\sum_{n=1}^{N-1} a_n \int_{-1}^{1} p_n(t) e^{jd \cdot t} dt = \sum_{n=1}^{N-1} a_n \sum_{j=1}^{N} \tilde{w}_j p_n(t_j), \; n = 0, .., N-1. \tag{9}$$

For this goal, we have to fulfill

$$\int_{-1}^{1} e^{jd \cdot t} p_n(t) dt = \sum_{j=1}^{N} \tilde{w}_j p_n(t_j), \; n = 0, .., N-1. \tag{10}$$

This leads to the generation of the linear system of equations

$$\begin{Bmatrix} p_0(t_1) & p_0(t_2) & \dots & p_0(t_N) \\ p_1(t_1) & p_1(t_2) & \dots & p_1(t_N) \\ \vdots & \vdots & \vdots & \vdots \\ p_{N-1}(t_1) & p_{N-1}(t_2) & \dots & p_{N-1}(t_N) \end{Bmatrix} \cdot \begin{Bmatrix} \tilde{w}_1 \\ \tilde{w}_2 \\ \vdots \\ \tilde{w}_N \end{Bmatrix} =$$

$$= \begin{Bmatrix} \int_{-1}^{1} p_0(t) e^{jd \cdot t} dt \\ \int_{-1}^{1} p_1(t) e^{jd \cdot t} dt \\ \vdots \\ \int_{-1}^{1} p_{N-1}(t) e^{jd \cdot t} dt, \end{Bmatrix}. \tag{11}$$

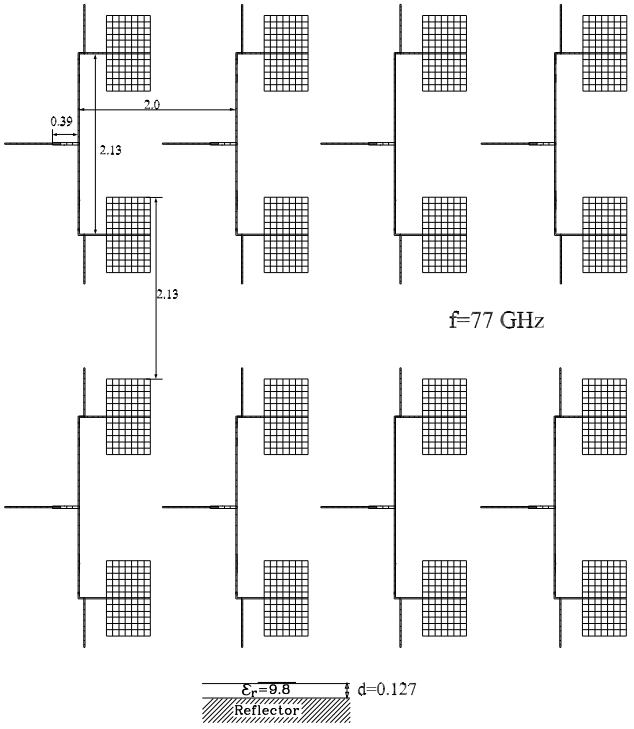

Fig. 2. Discretization of a 16-element patch array.

whose solution provides the integration weights $\tilde{w}_i$. The matrix has only to be computed once using the well known recurrence formula for the Legendre polynomials. Afterwards, we apply a LU-decomposition of this matrix with partial pivotisation and additional storage of a pivot index vector.

Thus the efficient computation of the right hand side of Eq. (11) forms the crucial point for the weight determination.

Here the main task is to solve

$$T_n(d) = \int_{-1}^{1} t^n e^{jd \cdot t} dt = \frac{1}{jd} t^n e^{jd \cdot t} \Big|_{-1}^{1} - \frac{n}{jd} \int_{-1}^{1} t^{n-1} e^{jd \cdot t} dt \tag{12}$$

by a recurrence relation. For the first term right hand side in Eq. (12), we get

$$\frac{1}{jd} t^n e^{jd \cdot t} \Big|_{-1}^{1} = \begin{cases} \frac{2}{d} \sin(d), & n \text{ even} \\ \frac{2}{jd} \cos(d), & n \text{ odd} \end{cases}. \tag{13}$$

Nevertheless, for $d < 0.5$ the computation with Eqs. (12) becomes unstable due to cancellation effects. In these cases, we compute the $T_n(d)$ with an iterative procedure using the power series representation of the complex exponential function, leading to compact series representations with very fast convergence. Using the weights $\tilde{w}_i$ allows to integrate the function $f(k_x)$ exactly up to polynomials of order $N-1$ providing a much higher accuracy than with classical Filon integration rules. Since we use a similar basic principle, our method may be called Legendre-Filon quadrature.

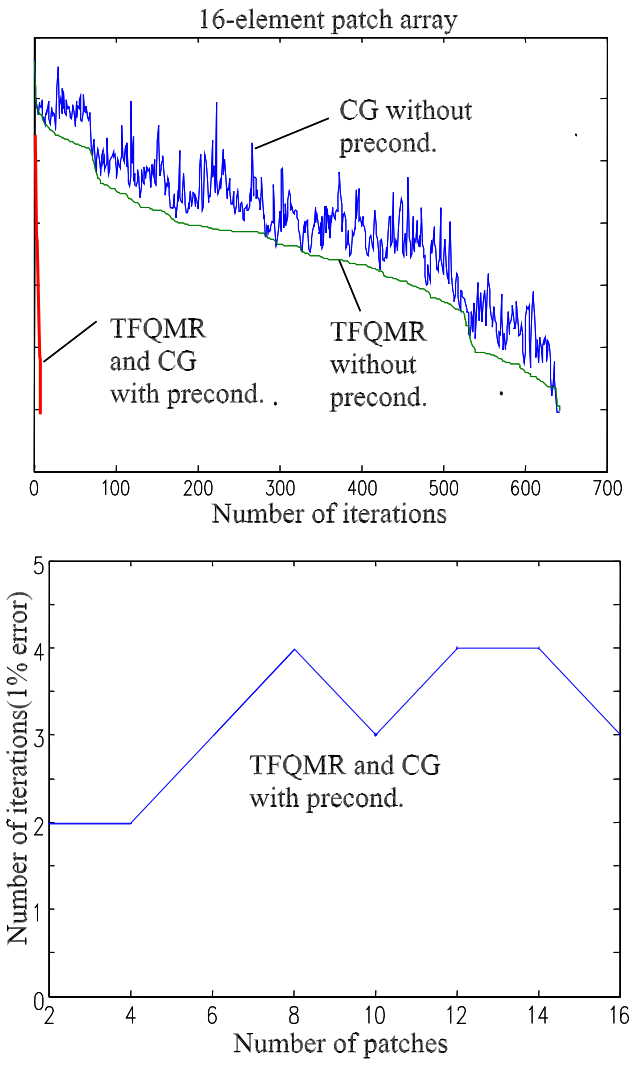

Fig. 3. Solution behavior of 16-element patch array. Top: Convergence history. Bottom: Iteration number in dependence on the number of patches.

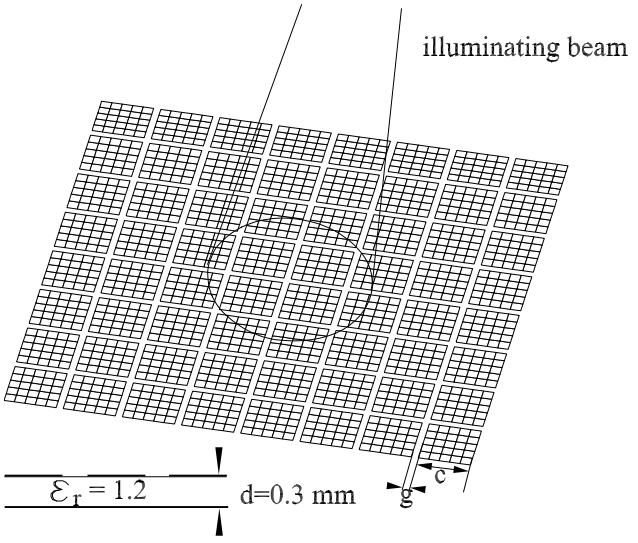

Fig. 4. Multibeam antenna array as part of an astronomical telescope. g=0.15 mm, c=1.1 mm.

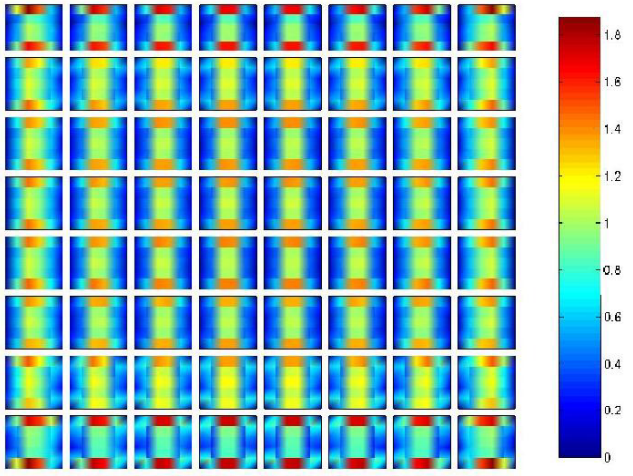

Fig. 5. Current distribution (A/mm) of a multibeam antenna excited by an incident plane wave at f=250 GHz.

The effort for computing the weights can be further reduced by using a composite Legendre-Filon integration. This means that the sampling points are subdivided into several intervals whereas the weights are only computed for the first intervall. The weights for the other intervalls are simply derived from the weights of the first intervall by multiplying them with a fixed exponential term.

3 Applications

As first application we present the analysis of a 16-element patch array consisting of 2-element subarrays. Figure 2 shows the dimensions and discretization of the structure.

The structure was discretited with 2400 basis functions. For the matrix decomposition, we introduced 40 ports leading to 48 blocks.

The solution behavior is given in Fig. 3. Figure 3 top shows the convergence history with a Transpose Quasi Minimum Residual (TFQMR) method and a standard CG-method. Without preconditioning the CG-method shows a strong oscillatory residual error whereas the TFQMR-method exhibits a smooth decay. With preconditioning, both methods show a very fast decay with only three necessary iterations for a residual error of 1%. Figure 3 bottom shows the necessary number of iterations (1% error) in dependence on the number of patches. We observe a nearly constant number of necessary iterations, thus the solution performance of our preconditioner is nearly independent on the number of unknowns.

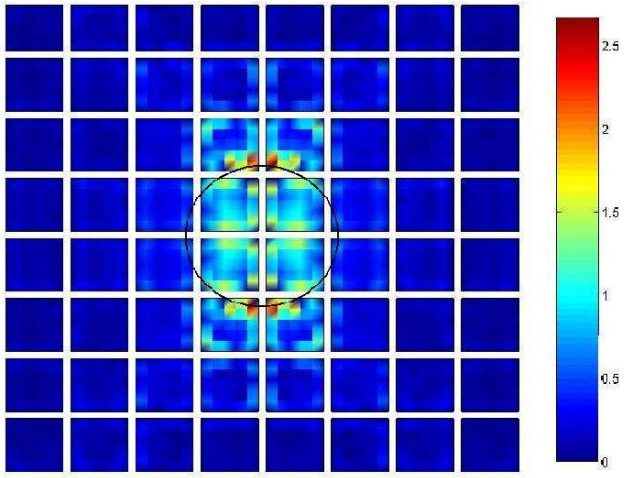

Fig. 6. Current distribution of a multibeam antenna excited by an incident plane wave only illuminating a circular region with diameter 3.05 mm.

A so-called multibeam antenna we present as a second application. It is intended as part of astronomical telescopes for image processing purposes in the submm-wave region. As given in Fig. 4, it consists of 64 patch elements mounted on a foam layer ($\epsilon_r \approx 1.2$) with reflector. We applied a discretization with 2560 unknowns. The lateral dimension of the structure amounts to about 12 wavelength at 250 GHz. For the preconditioning, each antenna element was assigned to one block at first, but we also assigned two elements to one block. The two-element blocks can be considered as isolated or we can introduce so-called virtual ports between the elements. With virtual ports between successive elements e.g. in each row, the elements of a row are considered as connected by current coupling although only field coupling exists between the elements. This leads to overlapping matrices similar as in in Eq. (3). Nevertheless, the performance of this preconditioning strategies is nearly the same and leads to about 11 iteration using a perpendicular plane wave excitation (E-field in x-direction with 1000 V/cm) over the whole array (Fig. 5). If we only illuminate a circular region of the array (Fig. 6), we need up to 24 iterations which can be traced back on the inhomogeneous excitation situation.

4 Conclusions

An optimized system matrix decomposition adapted to the topology of complex (M)MIC-structures was presented, leading to high performance preconditioners within Krylov subspace solvers. Using adaptive Cholesky decompositions and forward/backward substitutions, the computational and storage effort for the solution process of the linear systems of equations could be minimized. For the very accurate evaluation of the system matrix entries a Legendre-Filon integration technique was applied to the often highly oscillatory spectral domain integrands formulated in Cartesian wavenumbers. The methods were applied to microstrip array antennas and multibeam reflectarrays and have demonstrated excellent performance for both the matrix fill and the linear equation solution process.

References

Ooms, S. and De Zutter, D.: A New Iterative Diakoptics-Based Multilevel Moments Method for Planar Circuits, IEEE Trans. on Microwave Theory and Techn., 46, 3, 280–291, 1998.

Vaupel, T., Hansen, V., and Schäfer, F.: Radiation Efficiency Analysis of Submm-Wave Receivers Based on a Modified Spectral Domain Technique, Radio Science, 38, 4, 2003.

Vaupel, T. and Hansen, V.: Integralgleichungsanalyse von (M)MIC-Strukturen mit modifizierter Spektralbereichsintegration und diakoptischen Strategien, Kleinheubacher Berichte, 2001.

Vaupel, T. and Hansen, V.: Anwendungen einer modifizierten Spektralbereichsintegration für implizite Multilevelstrategien und detaillierte Abstrahlungsanalysen, Kleinheubacher Berichte, 2002.

Filon, L. N. G.: On a quadrature formula for trigonometric integrals, Proc. Roy. Soc. Edinburgh, 49, 38–47, 1928.

Pilz, D. and Menzel, W.: Mixed Integration Method for the Evaluation of the Reaction Integrals Using the Spectral Domain Method, IEE Proc. Microw. Antennas Propagation, 146, 3, 1999.